Tellus
SERIES B
CHEMICAL
AND PHYSICAL
METEOROLOGY
PUBLISHED BY THE INTERNATIONAL METEOROLOGICAL INSTITUTE IN STOCKHOLM

Tellus (2011), 63B, 77–85

TELLUS

The vertical distribution of thin features over the Arctic analysed from CALIPSO observations

Part I: Optically thin clouds

By ABHAY DEVASTHALE[1],* MICHAEL TJERNSTRÖM[2], KARL-GÖRAN KARLSSON[1], MANU ANNA THOMAS[3], COLIN JONES[4], JOSEPH SEDLAR[2] and ALI H. OMAR[5], [1]*Remote Sensing Division, Swedish Meteorological and Hydrological Institute, Folkborgsvagen 1, 60176 Norrköping, Sweden;* [2]*Department of Meteorology, Stockholm University, Stockholm, Sweden*; [3]*School of Environmental Sciences, University of East Anglia, Norwich, UK*; [4]*Rossby Center, Swedish Meteorological and Hydrological Institute, Norrköping, Sweden*; [5]*Science Directorate, NASA Langley Research Center, Hampton, Virginia, USA*

(Manuscript received 21 April 2010; in final form 25 October 2010)

ABSTRACT

Clouds play a crucial role in the Arctic climate system. Therefore, it is essential to accurately and reliably quantify and understand cloud properties over the Arctic. It is also important to monitor and attribute changes in Arctic clouds. Here, we exploit the capability of the CALIPSO-CALIOP instrument and provide comprehensive statistics of tropospheric thin clouds, otherwise extremely difficult to monitor from passive satellite sensors. We use 4 yr of data (June 2006–May 2010) over the circumpolar Arctic, here defined as 67–82°N, and characterize probability density functions of cloud base and top heights, geometrical thickness and zonal distribution of such cloud layers, separately for water and ice phases, and discuss seasonal variability of these properties. When computed for the entire study area, probability density functions of cloud base and top heights and geometrical thickness peak at 200–400, 1000–2000 and 400–800 m, respectively, for thin water clouds, while for ice clouds they peak at 6–8, 7–9 and 400–1000 m, respectively. In general, liquid clouds were often identified below 2 km during all seasons, whereas ice clouds were sensed throughout the majority of the upper troposphere and also, but to a smaller extent, below 2 km for all seasons.

1. Introduction

The Arctic climate system has undergone rapid changes in the recent few decades, primarily driven by increasing anthropogenic emissions (Gillett et al., 2008; Shindell and Faluvegi, 2009). These changes have been amplified by various feedback mechanisms. For example, the Arctic temperature has been increasing more than twice the global average since the mid-1960s (ACIA, 2005). The role of clouds with respect to both short-term changes (Kay and Gettelman, 2009) and long-term changes (Liu et al., 2009a) in the Arctic climate is vital as clouds are radiatively and dynamically coupled to every aspect of the Earth System (see Curry et al., 1996, for a comprehensive overview). However, our limited understanding of cloud properties along with a poor representation in climate models has contributed large uncertainties in estimating future climate change. This is especially true for the Arctic region (Tjernström et al., 2008), where ground-based observations are very sparse, and space-based observations from passive remote sensing instruments have limited capabilities (e.g. Karlsson and Dybbroe, 2009).

Recently, the need is expressed to identify, and more importantly, to characterize the various cloud regimes that are likely most susceptible to the influence of aerosols originating from anthropogenic activities (Stevens and Feingold, 2009). One such cloud category is low-level optically and geometrically thin clouds in the Arctic (see Turner et al., 2007, for an overview). It has been suggested that the part of the recent warming over the Arctic is due to changes in the aerosol regimes (Shindell and Faluvegi, 2009), which in turn may affect thin clouds and enhance or diminish the trends. Various mechanisms with which aerosols can affect clouds in the Arctic have been proposed (Blanchet and Girard, 1994; Garrett and Zhao, 2006; Lubin and Vogelmann, 2006). Large solar zenith angles in summer and the absence of solar radiation in winter result in the long-wave component of cloud forcing being dominant for most part of the year (Walsh and Chapman, 1998). Hence, aerosol indirect effects in

*Corresponding author.
e-mail: Abhay.Devasthale@smhi.se
DOI: 10.1111/j.1600-0889.2010.00516.x

the long-wave spectrum are especially important for the Arctic region (Garrett et al., 2002; Garrett and Zhao, 2006; Lubin and Vogelmann, 2006). Aerosols impact the emissivity of thin water clouds by increasing the infrared optical depth of thin water clouds and may thus change the long-wave radiation re-emitted towards the surface (Garrett et al., 2002). It is therefore essential to quantify the properties of such clouds so as to fully assess their susceptibility to changes in aerosol loadings.

Detection of optically and geometrically thin clouds present a challenge for passive instruments, especially when the surface below is snow and ice and/or very cold as is often the case in the Arctic (Karlsson and Dybbroe, 2009). The data from the Cloud-Aerosol Lidar with Orthogonal Polarization (CALIOP) instrument onboard Cloud-Aerosol Lidar and Infrared Pathfinder Satellite Observation (CALIPSO) satellite (Winker et al., 2009) provides an unprecedented opportunity to investigate these clouds at very high vertical resolution, due to its strong sensitivity to clouds with optical thickness less than 5. This paper is first of the two-part series where we exploit this capability of CALIPSO-CALIOP. In this paper we provide comprehensive statistics on optically thin cloud properties over the circumpolar Arctic, here defined as 67–82°N (Note that the satellite coverage is limited to $<\sim$82°N). We herein compute probability density functions (PDFs) of cloud top and base heights as well as geometrical thickness, for water and ice phase cloud layers separately and also discuss seasonal variations. We also present the zonal distributions of water and ice clouds. In the companion paper (Devasthale et al., 2011), we present similar statistics for aerosols over the same region and time period.

The paper is organized as follows. In Section 2, we briefly discuss the data used, followed by a discussion of results in Section 3. Summary and conclusions are provided in Section 4.

2. CALIOP data

In the present analysis, we used the recently released standard CALIPSO 5 km Cloud Layer Version 3 product. The details of CALIPSO products, algorithms and their validations can be found in Hu et al. (2009), Liu et al. (2009b), Vaughan et al. (2009), Winker et al. (2009) and Young and Vaughan (2009). A snapshot of the CALIOP curtain over the Arctic is shown in Fig. 1. The top panel shows 532 nm attenuated backscatter, whereas middle and bottom panels show corresponding depolarization ratios and vertical feature mask. In the first image, the warm colours (red to white) denote high-attenuated backscatter corresponding to clouds whereas the lower attenuated

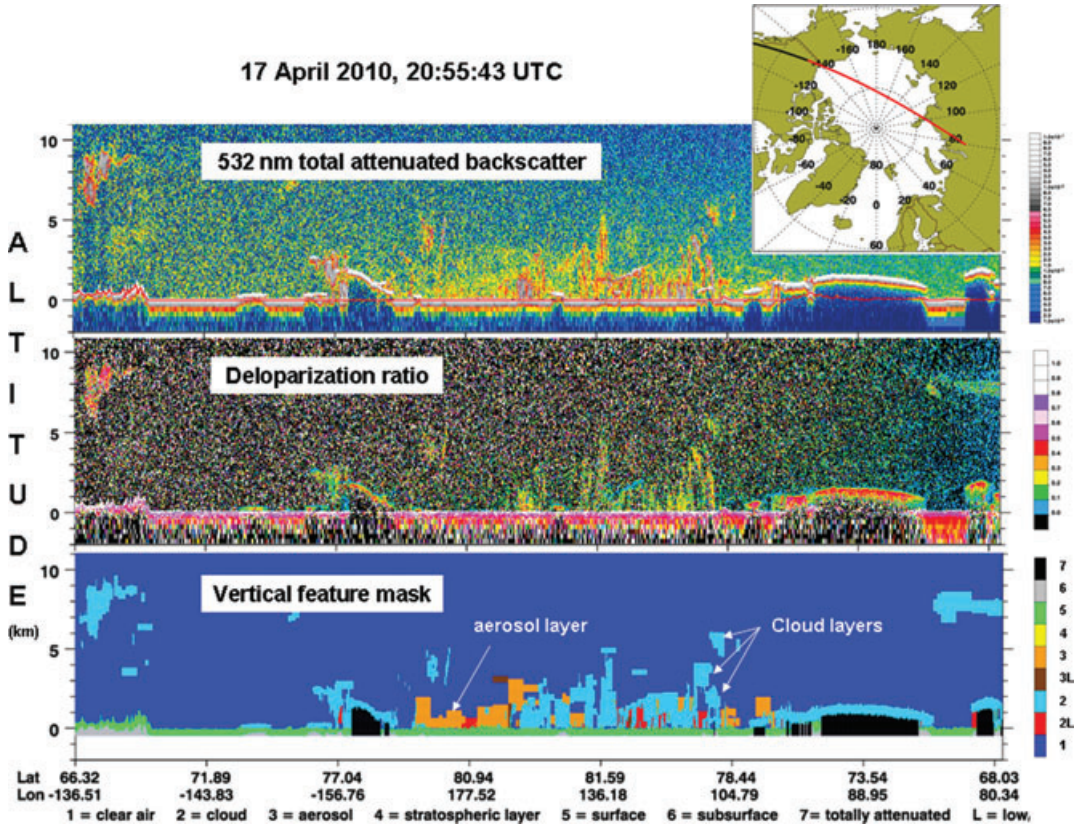

Fig. 1. A snapshot of CALIOP curtain over the Arctic. The top panel shows vertically resolved 532 nm attenuated backscatter, whereas middle and bottom panels show corresponding depolarization ratio and vertical feature mask.

backscatter (yellow to blue) corresponds to aerosols and clear air as illustrated by the vertical feature mask in the lower panel. The middle panel is a plot of the volume depolarization ratio used to discriminate between aerosols and clouds (Liu et al., 2009) and identify aerosol subtypes (Omar et al., 2009). CALIPSO observes a significant amount of high depolarization ratio particles near the surface, which is labelled cloud but are more likely diamond dust or ice fog.

A rigorous quality control is applied by selecting only high confidence estimates for the analysis. For example, based on the information in the feature classification flags, the retrievals are used only if: (a) the feature is classified as cloud; (b) The quality of the feature classification is set to 'high' and (c) the cloud phase discrimination quality (Hu et al., 2009) is also set to 'high'. The data used here cover a 4-yr period from June 2006 to May 2010. Data are analysed for the four seasons separately, winter (December, January and February; DJF), spring (March, April and May; MAM), summer (June, July and August; JJA) and autumn (September, October and November; SON).

The lidar signal becomes substantially saturated as cloud optical thickness increases more than 3, and becomes fully saturated above 5. Thus, the statistics presented here are essentially for clouds with optical depths less than 3, which is the main aim of this study. Given this limit on optical depth, the cloud types that would be analysed here are transparent cirrus, low-level overcast partly transparent clouds, transition stratocumulus, transparent altocumulus, etc. The cloud layers in which the lidar signal was fully attenuated, and thus cloud base information was not retrieved, are discarded in the analysis. Clouds categorized in either water or ice phases are analysed. At the time of this writing, the information on the mixed-phase clouds was missing in the CALIPSO 5 km layer products. Previous studies have shown that the mixed-phase clouds are present over the Arctic, although full characterization over the entire Arctic Ocean is lacking, and information is limited to only few locations (Shupe et al., 2006; Verlinde et al., 2007; de Boer et al., 2009; Ehrlich et al., 2009; Gayet et al., 2009). Such clouds may have been classified in liquid or ice categories in our analysis depending upon the dominant phase of condensate. The lidar retrievals below 100 m can be sometimes noisy and hence due care is taken to avoid such cases using quality flags. It should finally be noted here that observations poleward of $\sim 82^{\circ}$ are not available due to CALIPSO's orbital configuration.

Figure 2 shows the total number of cloud layers finally used for the analysis for each season, while at the same time providing an overview of the study domain. It is worth noting that the

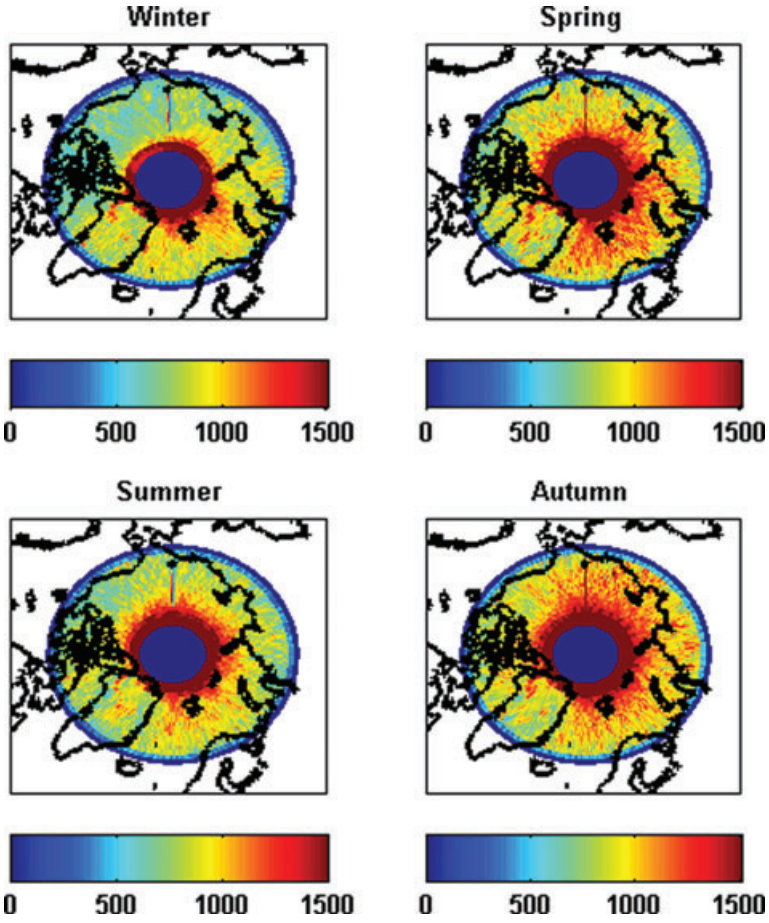

Fig. 2. Total number of observations used in the analysis for four seasons (June 2006–May 2010) after applying high-quality flags mentioned in Section 2.

distribution is far from homogeneous. In winter and spring, there is a strong bias in the data distribution towards the very highest latitudes and also towards the northern North Atlantic sector. In summer and autumn, the distribution is more homogeneous in general, but still with a bias to more northerly locations. The presence of Greenland, with its special properties, is also quite obvious in the plots.

3. Results and discussions

Figure 3 presents the relative distribution of the number of cloud layers over the whole study area. The clear sky fraction is largest in winter at ∼28%, and smallest in autumn at ∼17%. In general, single-layer only clouds occur about 35–45% of the time, whereas two-layer cloud systems occur around 20% of the time. Multiple layered cloud systems, with up to six to seven layers, also occur frequently. In a previous study, Intrieri et al. (2002) reported occurrence of up to five cloud layers using 1-yr of ground-based remote sensing measurements over the Surface Heat Budget of the Arctic (SHEBA) area (Uttal et al., 2002). The occurrence of multilayered clouds during SHEBA was larger than that for single layer clouds in June and July. A direct comparison with their results is difficult because we analysed the seasonal statistics over much larger area and for a different time period.

Figures 4 and 5 show zonal distributions of water and ice phase clouds, respectively, and their seasonal variability. The bin size is 200 m in the vertical (y-axis) and 1° in the zonal direction (x-axis). In each longitude-height bin, all the observations in Fig. 2 are aggregated according to height and location. Also note the dome-like structure around 20–60°W is due to the Greenland topography. Water clouds (Fig. 4) show strong intraannual variability within the lowermost 2 km in the troposphere. Here it is necessary to take into account the role of synoptic-scale weather patterns over the study area when interpreting the results, because they will have first-order influence on the regional distribution of cloud amount and type. In winter, the semi-permanent Icelandic low brings cyclones up to the Norwegian, Greenland and Barents Seas. This is the most dominating feature that governs the cloud distribution over the study area, clearly reflected for the winter and spring cases in Fig. 4. In contrast, the Siberian and Beaufort highs lead to much lower cloud amounts. In summer, however, the contrast between these semi-permanent highs and lows weakens considerably, resulting into more uniform distribution of low-level water clouds along the Arctic Circle. This is also well reflected in Fig. 4. In spring and autumn, the areas of northern Alaska, East Siberian Sea, Chukchi Sea and Beaufort Sea extending into the Arctic Ocean show relatively high low-level thin water cloud amounts compared to other seasons. The annual variability of the sea ice distribution is also important as is the distribution of land and sea in the study domain. Although snow and ice surfaces dominate in winter, the northern North Atlantic sector of the domain is largely ice free in summer while the North Pacific sector, for example, likely has more influence from sea ice. This, however, is rapidly changing, as this is the sector where most of the recent increase in melt has occurred.

Cirrus clouds dominate the distribution of thin ice clouds in the upper troposphere for all seasons (Fig. 5). One noticeable feature seen in the zonal distribution is the change in the heights and amounts of these clouds over Greenland, which gradually smears out eastwards in winter and spring seasons. The role of waves in the predominantly westerly flow across Greenland, especially during positive phases of Arctic Oscillation (AO), is

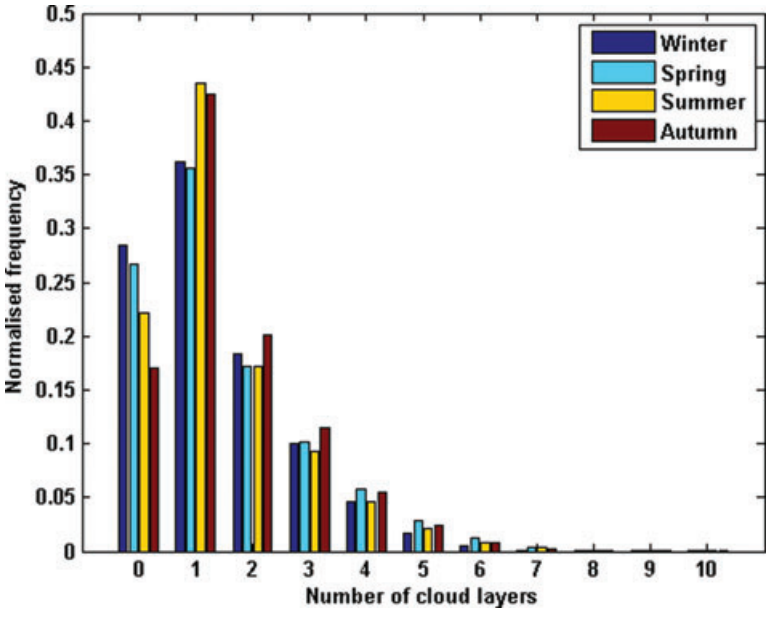

Fig. 3. Relative frequency of the number of cloud layers over the study area (67–82N) and their seasonal variations.

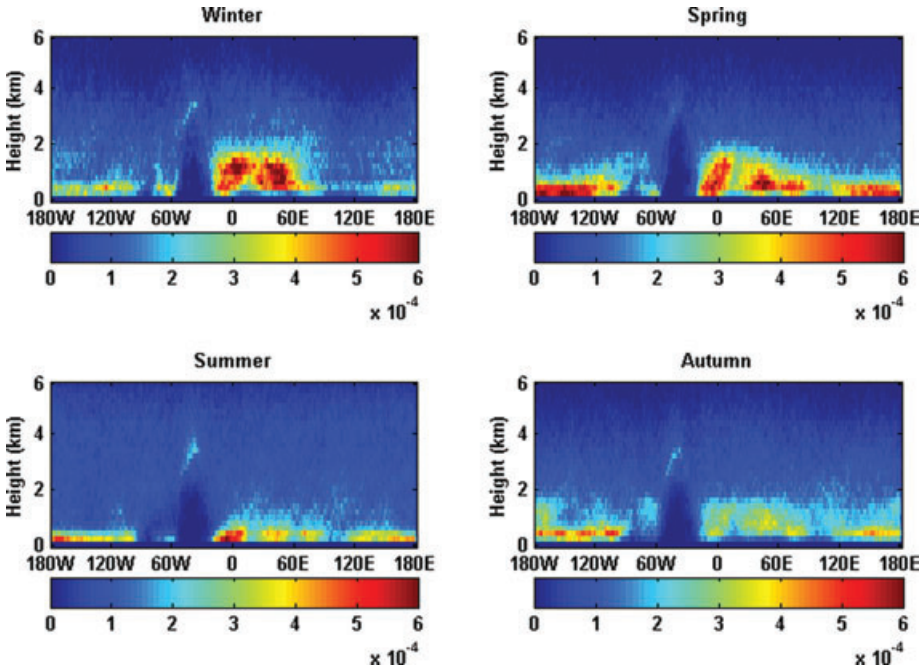

Fig. 4. The zonal distribution of water phase clouds and their seasonal variations. The height on *Y*-axis is in km. The observations over the 67–82N are aggregated for each bin, and each bin is normalized by the total number of observations in the entire joint histogram.

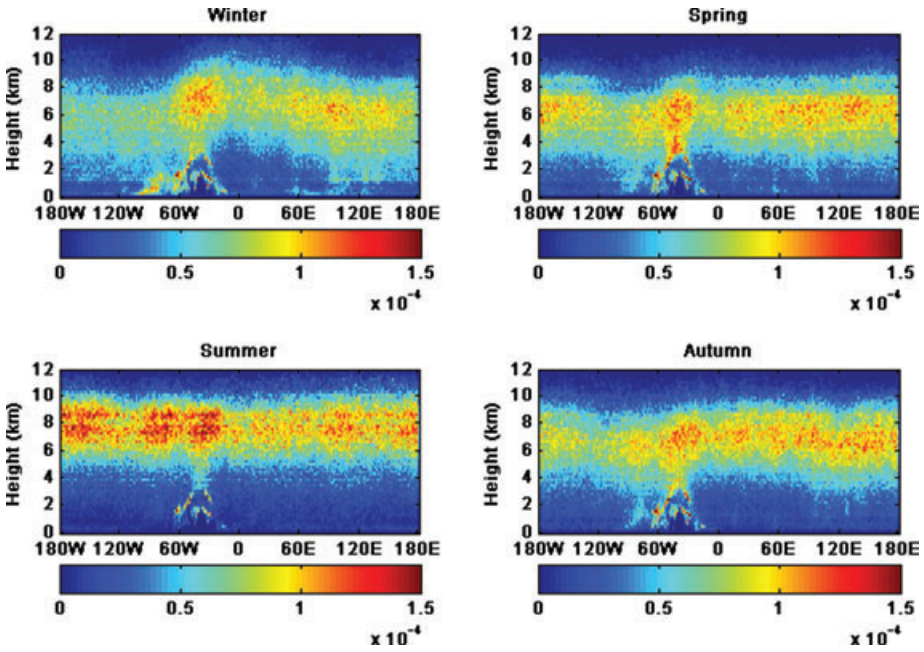

Fig. 5. Same as in Fig. 1, but for ice phase clouds.

crucial. The centre of action of the AO is usually situated over the northern Greenland at 100 hPa and over the southern Greenland at 500 hPa. Strong winds passing over Greenland generate buoyancy waves that propagate to the upper troposphere and lower stratosphere region leading to such a pattern. In winter, significant fractions of thin ice clouds are also observed in the lower troposphere over the eastern Canadian archipelago, Greenland and to some extent over parts of the Greenland and Barents Seas.

The thermodynamic phase of a thin cloud, its vertical position in the atmosphere and its seasonal variability has varying impact on the radiative fluxes in the atmosphere and the surface. Moreover, the relative frequency of occurrence of water and ice

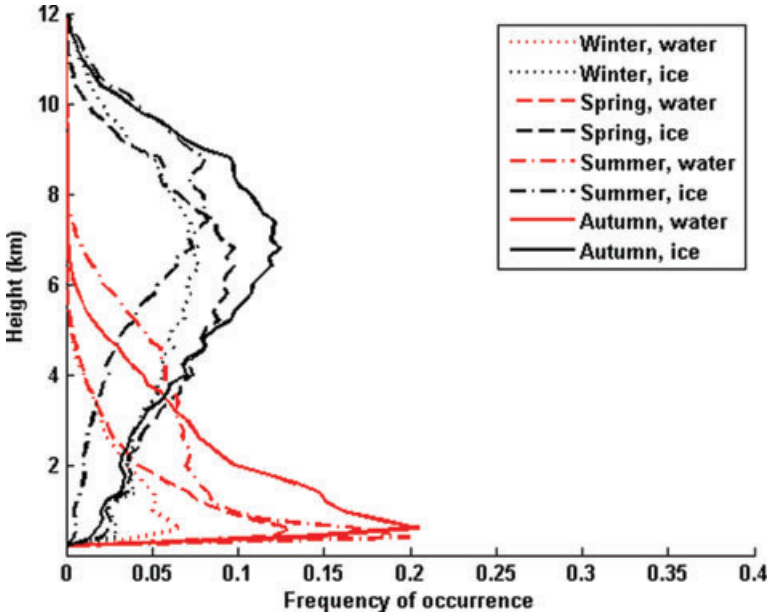

Fig. 6. The frequency of occurrence of water and ice phase clouds. Note that only those observations that satisfy high-quality criteria given in Section 2 are used for the analysis.

clouds, especially in the lowermost troposphere, has strong influence on the radiation reaching the surface in the Arctic due to different refractive indices of water droplets and ice crystals. The relative vertical distribution would also have influence on their susceptibility to aerosols, thus further adding complexity in determining their overall role in aerosol–cloud interactions in the Arctic. The frequency of occurrence of water and ice phase clouds for different seasons as a function of height is shown in Fig. 6. Vertical distribution of water phase clouds show that their occurrence is largest in autumn followed by summer, spring and winter. Liquid water clouds are as expected most prominent in the lower troposphere, mostly below 1–2 km. Interestingly, in the lowermost troposphere (up to 400 m), a significant presence of both ice and liquid is observed in all seasons. This is consistent with observations from SHEBA, showing liquid water in low clouds at very low temperatures and from the Arctic Summer Cloud Ocean Study (ASCOS) campaign showing prevailing low-level mixed-phase clouds at relatively high summer temperatures. There are, however, also several problems with CALIOP measurements of ice phase clouds at these levels. For example, in winter, apart from ice clouds there is a possibility that CALIOP is detecting boundary-layer ice crystals (Wilson et al., 1993; Bourdages et al., 2009), ice fog, diamond dust or ice precipitation (Clark et al., 1996) falling below thin water clouds (Intrieri and Shupe, 2004) or combination of these phenomena. The zonal distribution shows that the Canadian archipelago contributes mostly to the ice phase clouds in the lowermost troposphere (Fig. 5). As this is rugged terrain there is a possibility that the snow or ice crystals blown by wind from such terrain could be detected by CALIOP (Lesins et al., 2009). Although all of these phenomena are reported to be present in the Arctic, there is still not enough literature available to establish their relative importance covering the entire Arctic region.

The PDFs of cloud base and cloud top heights are shown in Fig. 7. The PDFs for both water and ice clouds are skewed. The PDFs for cloud base height of water clouds peak in the two lowermost bins (i.e. below 400 m) in all seasons. The PDFs for water clouds in summer are very broad compared to other seasons. There is also a clear seasonality in the PDFs of cloud base height between summer and winter months, with the PDF peaking sharply around 200–400 m in winter, whereas in summer, the PDF is quite broad additionally showing substantial amount of clouds with bases at around 2–4 km. This is somewhat unexpected in the light of many earlier studies showing that summer is dominated by low clouds (e.g. Intrieri et al., 2002; Tjernström et al., 2004). A possible reason for this is that the domain in this study includes significant land areas whereas many earlier studies are over the ice-covered ocean. Over land in summer higher cloud bases in summertime convection could be expected. The PDFs of top height for water clouds peak around 1–2 km in line with the expected predominance of low water clouds. Interestingly, the liquid clouds above 2 km in summer and autumn are geometrically thinner than those found in winter and spring. Thus, the vertical distribution of cloud liquid water content, as well as liquid droplet radius, will have a distinct influence on the radiative transfer through such clouds. The PDFs of cloud base height for ice phase clouds are broad but peak at around 6–8 km, whereas for cloud tops they peak around 7–9 km.

Figure 8 shows the PDFs of cloud geometrical thickness. The distributions for both water and ice phase clouds are positively skewed, with broader distributions for ice-phase clouds than for liquid phase clouds. The seasonal variations in the peaks of PDFs are clearly visible. The geometrical thickness of thin

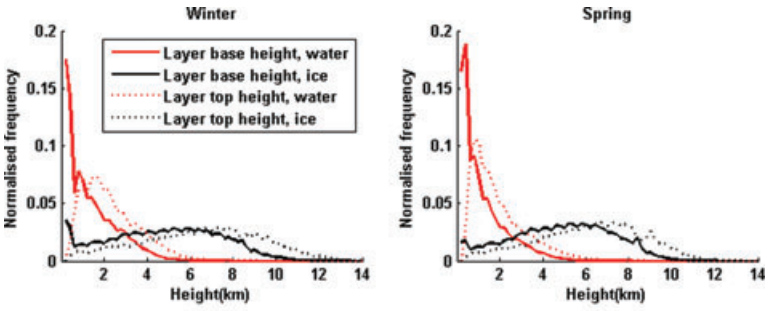

Fig. 7. Probability density functions (PDFs) of the cloud layer base and layer top heights for water and ice phase clouds and their seasonal variations.

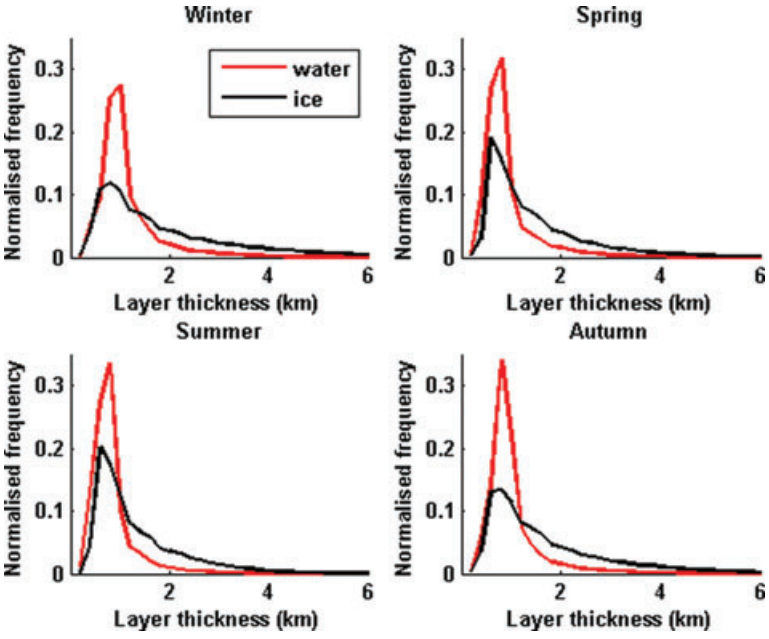

Fig. 8. PDFs of layer geometrical thickness for water and ice phase clouds, and their seasonal variations.

liquid-phase clouds peaks around 400–800 m, whereas for ice-phase clouds, the PDFs peak around 400–1000 m. In winter, geometrically very thick but optically thin ice clouds (predominantly cirrus) are also observed in many cases. A qualitative comparison with the results from previous studies using lidar/radar observations at few stations or from observational campaigns over the Arctic shows generally good agreement with our results. For example, Intrieri et al. (2002), using radar-lidar data for the period of 1-yr over the SHEBA area, provide histograms of the lowest cloud base height that peak in the lowermost 1-km bins for all seasons. Sedlar and Tjernström (2009) identified single-layer clouds with cloud top below 2.2 km occurring across 60% of the time during late summer from the Arctic Ocean Expedition 2001. Dong and Mace (2003) also report cloud base heights of Arctic stratus over the ground station at Barrow, Alaska, in the lowermost 1 km for the summer 2000.

4. Conclusions

We provide, for the first time, extensive statistics on optically thin water and ice clouds over a large part of the Arctic using the CALIPSO data for the period June 2006 through May 2010.

The CALIOP instrument is ideally suited to study optically thin clouds (with optical depth <3), especially over the Arctic where such clouds are present in significant amounts in the lowermost troposphere. These clouds are also susceptible to the aerosol influence in the Arctic, and hence accurate information on their characteristics is needed to assess the impact of a changing aerosol climate. In this study, we have characterized PDFs of cloud base and top heights, geometrical thickness and zonal distribution of such cloud layers separately for water and ice clouds and discussed seasonal variability of these properties. The PDFs are in general broad and long-tailed. When computed for the entire study area, the PDFs of cloud base and top heights and geometrical thickness peak at 200–400, 1000–2000 and 400–800 m, respectively, for thin water clouds, whereas for ice clouds, they peak at 6–8 km, 7–9 km and 400–1000 m, respectively. The zonal distribution of thin water and ice clouds shows the footprints of major synoptic weather patterns (i.e. semi-permanent highs and lows, Arctic Oscillation) in the regional distribution of clouds over the Arctic. When the CALIOP data set becomes longer it would be interesting to investigate interannual variations, and correlations of some of these findings with the AO index variations (e.g. Wang and Key 2005). At the present this is not possible due to the length of the satellite data record.

5. Acknowledgments

The authors gratefully acknowledge the CALIPSO Science Team and NASA Langley Atmospheric Science Data Center (ASDC) for making data freely available for research. This work was supported by the Swedish National Space Board.

References

Arctic Climate Impact Assessment (ACIA). 2005. *Arctic Climate Impact Assessment*. Cambridge University Press, 1042 pp. Available at: http://www.acia.uaf.edu/pages/scientific.html. Accessed: 2 September 2009.

Blanchet, J.-P. and Girard, E. 1994. Arctic greenhouse cooling. *Nature* **371**, 383.

Bourdages, L., Duck, T. J., Lesins, G., Drummond, J. R. and Eloranta, E. W. 2009. Physical properties of High Arctic tropospheric particles during winter. *Atmos. Chem. Phys.* **9**, 6881–6897.

Clark, M. P., Serreze, M. C. and Barry R. G. 1996. Characteristics of Arctic Ocean climate based on COADS data, 1980–1993. *Geophys. Res. Lett.* **23**(15), 1953–1956.

Curry, J. A., Rossow, W. B., Randall, D. and Schramm, J. L. 1996. Overview of Arctic cloud and radiation characteristics. *J. Clim.* **9**, 1731–1764.

de Boer, G., Eloranta, E. W. and Shupe, M. D. 2009. Arctic mixed-phase stratiform cloud properties from multiple years of surface-based measurements at two high-latitude locations. *J. Atmos. Sci.* **66**, 2874–2887.

Devasthale, A., Tjernström, M. and Omar, A. H. 2011. The vertical distribution of thin features over the Arctic analyzed from CALIPSO observations. Part II – aerosols. *Tellus* **63B** this issue.

Dong, X. and Mace, G. G. 2003. Arctic stratus cloud properties and radiative forcing derived from ground-based data collected at barrow, Alaska. *J. Clim.* **16**, 445–461.

Ehrlich, A., Wendisch, M., Bierwirth, E., Gayet, J.-F., Mioche, G. and co-authors. 2009. Evidence of ice crystals at cloud top of Arctic boundary-layer mixed-phase clouds derived from airborne remote sensing. *Atmos. Chem. Phys. Discuss.* **9**, 13801–13842.

Garrett, T. J., Radke, L. F. and Hobbs, P. V. 2002. Aerosol effects on the cloud emissivity and surface longwave heating in the Arctic. *J. Atmos. Sci.* **59**, 769– 778.

Garrett, T. J. and Zhao, C. 2006. Increased Arctic cloud longwave emissivity associated with pollution from mid-latitudes. *Nature* **440**, 10.1038/nature04636, 787–789.

Gayet, J-F., Mioche, G., Dörnbrack, A., Ehrlich, A., Lampert, A. and co-authors. 2009. Microphysical and optical properties of Arctic mixed-phase clouds – the 9 April 2007 case study. *Atmos. Chem. Phys.* **9**, 6581–6595.

Gillett, N. P., Stone, D. A., Stott, P. A., Nozawa, T., Karpechko, A. Yu. and co-authors. 2008. Attribution of polar warming to human influence. *Nat. Geosci*. **1**, 750–754, doi:10.1038/ngeo338.

Hu, Y., Winker, D., Vaughan, M., Lin, B., Omar, A. and co-authors. 2009. CALIPSO/CALIOP cloud phase discrimination algorithm. *J. Atmos. Ocean. Tech.* **26**, 2293–2309.

Intrieri, J. M., Shupe, M. D., Uttal, T. and McCarty, B. J. 2002. An annual cycle of Arctic cloud characteristics observed by radar and lidar at SHEBA. *J. Geophys. Res.* **107**(C10), doi:10.1029/2000JC000423.

Intrieri, J. M. and Shupe, M. D. 2004. Characterization and radiative effects of diamond dust of the Western Arctic Ocean region. *J. Clim.* **17**, 2953–2960.

Karlsson, K.-G. and Dybbroe, A. 2009. Evaluation of Arctic cloud products from the EUMETSAT Climate Monitoring Satellite Application Facility based on CALIPSO-CALIOP observations. *Atmos. Chem. Phys.* **9**, 1687–1709.

Kay, J. E. and Gettelman, A. 2009. Cloud influence on and response to seasonal Arctic sea ice loss. *J. Geophys. Res.* **114**, D18204, doi:10.1029/2009JD011773.

Lesins, G., Bourdages, L., Duck, T. J., Drummond, J. R., Eloranta, E.W. and co-authors. 2009. Large surface radiative forcing from topographic blowing snow residuals measured in the High Arctic at Eureka. *Atmos. Chem. Phys.* **9**, 1847–1862.

Liu, Y., Key, J. and Wang, X. 2009a. Influence of changes in sea ice concentration and cloud cover on recent Arctic surface temperature trends. *Geophys. Res. Lett.*, **36**, L20710, doi:10.1029/2009GL040708.

Liu, Z., Vaughan, M., Winker, D., Kittaka, C., Getzewich, B. and co-authors. 2009b. The CALIPSO lidar cloud and aerosol discrimination: Version 2 Algorithm and initial assessment of performance. *J. Atmos. Oceanic Tech.* **26**, 1198–1213.

Lubin, D. and Vogelmann, A. M. 2006. A climatologically significant aerosol longwave indirect effect in the Arctic. *Nature* **439**, 26 January, 453–456, doi:10.1038/nature04449.

Omar, A., Winker, D., Kittaka, C., Vaughan, M., Liu, Z. and co-authors. 2009. The CALIPSO automated aerosol classification and lidar ratio selection algorithm, *J. Atmos. Oceanic Technol.* **26**(10), 1994–2014.

Sedlar, J. and Tjernström, M. 2009. Stratiform cloud—inversion characterization during the Arctic Melt Season. *Boundary-Layer Meteorol.* **132**, 455–474, doi:10.1007/s10546-009-9407-1.

Shindell, D. and Faluvegi, G. 2009. Climate response to regional radiative forcing during the twentieth century. *Nat. Geosci.* **2**, 294–300, doi:10.1038/ngeo473.

Shupe, M. D., Matrosov, S. Y. and Uttal, T. 2006. Arctic mixed-phase cloud properties derived from surface-based sensors at SHEBA. *J. Atmos. Sci.* **63**, 697–711.

Stevens, B. and Feingold, G. 2009. Untangling aerosol effects on clouds and precipitation in a buffered system. *Nature* **461**, 607–613.

Tjernström, M., Leck, C., Persson, P. O. G., Jensen, M. L., Oncley, S. P. and co-authors. 2004. The summertime Arctic atmosphere: Meteorological measurements during the Arctic Ocean Experiment (AOE-2001). *Bull. Amer. Met. Soc.* **85**, 1305–1321.

Tjernström, M., Sedlar, J. and Shupe, M. D. 2008. How well do regional climate models reproduce radiation and clouds in the Arctic? An evaluation of ARCMIP simulations. *J. Appl. Met. Clim.* **47**, 2405–2422.

Turner, D. D., Vogelmann, M., Austin, R. T., Barnard, J. C., Cady-Pereira, K. and co-authors. 2007. Thin liquid water clouds: their importance and our challenge. *Bull. Amer. Meteor. Soc.*, 177–190.

Uttal, T., Curry, J. A., McPhee, M. G., Perovich, D. K., Moritz, R. E., and co-authors. 2002. Surface heat budget of the Arctic Ocean. *Bull. Amer. Meteor. Soc.* **83**, 255–275.

Vaughan, M., Powell, K., Kuehn, R., Young, S., Winker, D. and co-authors. 2009. Fully automated detection of cloud and aerosol layers in the CALIPSO lidar measurements. *J. Atmos. Oceanic Technol.* **26**, 2034–2050, doi:10.1175/2009JTECHA1228.1.

Verlinde, J., Harrington, J. Y., McFarquhar, G. M., Yanuzzi, V. T., Avramov, A. and co-authors. 2007. The mixed-phase Arctic cloud experiment. *Bull. Amer. Meteor. Soc.* **88**, 205–221.

Walsh, J. E. and Chapman, W. L. 1998. Arctic cloud–radiation–temperature associations in observational data and atmospheric reanalyses. *J. Clim.* **11**, 3030–3045.

Wang, X. and Key, J. 2005. Arctic surface, cloud, and radiation properties based on the AVHRR Polar Pathfinder data set. Part I: Spatial and temporal characteristics. *J. Clim.* **18**(14), 2558–2574.

Wilson, L. D., Curry, J. A. and Ackerman, T. P. 1993. Satellite retrieval of lower-tropospheric ice crystal clouds in the polar regions. *J. Clim.* **6**, 1467–1472.

Winker, D. M., Vaughan, M. A., Omar, A. H., Hu, Y., Powell, K. A., and co-authors. 2009. Overview of the CALIPSO Mission and CALIOP Data Processing Algorithms. *J. Atmos. Oceanic Technol.* **26**, 2310–2323, doi:10.1175/2009JTECHA1281.1.

Young, S. A. and Vaughan, M. A. 2009. The retrieval of profiles of particulate extinction from Cloud Aerosol Lidar Infrared Pathfinder Satellite Observations (CALIPSO) data: Algorithm description. *J. Atmos. Oceanic Technol.* **26**, 1105–1119, doi:10.1175/2008 JTECHA1221.1.